İSTANBUL UNIVERSITY CERRAHPAŞA

RESEARCH ARTICLE

Electrica 2020; 20(2): 182-188

Multifractal Behaviour of Respiratory Signals

Ertuğrul Saatçi, Esra Saatçi

Department of Electrical and Electronics Engineering, İstanbul Kültür University, İstanbul, Turkey

Cite this article as: Saatçi E, Saatçi E. Multifractal Behaviour of Respiratory Signals. *Electrica*, 2020; 20(2): 182-188.

ABSTRACT

In this study, to analyze the biomedical signals emerging from fractal structures in the human body, fractal analysis was used. Respiratory signals, such as airflow, mouth pressure, and lung volume, comprise a complex relationship that has not been inspected to date. Furthermore, the mechanism for which it is linked to the lung's fractal structure has not been scrutinized to date. Thus, using a well-known method, known as multifractal detrended fluctuation analysis (MF-DFA), this study aims to determine both mono- and multi-fractal property of respiratory signals ,. The real signals were analyzed using the MF-DFA algorithm. Moreover, for different scales, generalized Hurst exponent values were calculated. The results demonstrated that respiratory signals are fractional Brown motion-type signals, whereas fractal properties demonstrate less intersubject change. Moreover, in addition to both airflow and lung volume, respiratory signals and sounds are multifractal signals. In conclusion, the presence of the lung's long-memory property is the primary reason of multifractality.

Keywords: Generalized Hurst exponent, monofractal, multifractal, respiratory signals

Introduction

Fractal behavior is a scaling symmetry that defines a physical phenomenon's behavior. In a time series, this symmetry demonstrates as a statistical self-similarity at mulitple scales. At such time scales, statistically self-similar indicates that aspects of the time series demonstrate the same statistical properties. To obtain statistical self-similarity in a time series $x(t)$, the scaling time *t* using a factor of a may require scaling the values of $x(t)$ by a a^H factor. In the scaling relation $x(t) \rightarrow a^H x(at)$, H is known as the Hurst exponent. Moreover, it defines the type of self-similarity, e.g., if $x(t)$ is a trace of a Brownian motion defined by $H = 0.5$, the scaling time axis by a factor of four scales the signal by a factor of two. However, multiple time series do not exhibit the monofractal scaling behavior, in which a single scaling exponent is sufficient to describe the system's dynamics. For these cases, to define the scaling behavior, a multitude or an infinite number of scaling exponents must be used. Consequently, a multifractal analysis must be applied.

Recently, researchers demonstrated that many of the encountered time series demonstrate both mono- and multi-fractal properties. Thus, for scrutinizing the complexities of the time series, fractal analysis may be an effective approach . In this respect, in the human body, fractal analysis has been used to analyze the biomedical signals emerging from fractal structures. For identifying the characteristics of the complexities in the human body, techniques, such as electrocardiography and heart rate [1], electroencephalography and nerve conduction [2], [3], biomedical imaging [4], and respiratory sounds [5], are the best candidates . In these studies, as a tool to discover the parameters or features to determine and classify ailments, fractal analysis has been used.

Moreover, the fractal structure of lungs has been proven using the anatomical and morphological structures and gas dynamics of lungs [6]. In [7], the lung's fractal dimension was reported to be 2.88 using the lung's morphological structure. In both [5] and [8], respiratory sounds were shown to have information about the lung's fractal structure. , Moroever, the fractal dimension was estimated using different methods. In [9], [10], and [11], to distinguish the normal and abnormal lung sounds for diagnosis, fractal dimension was used. Moreover, it was used to detect and filter out heart sounds covered in lung sounds [10], [12].

Airflow, mouth pressure, and lung volume have a complex relationship in the form of impedance in electrical circuit models. However, how this complex relationship is linked to the lung's

Corresponding Author:
Ertuğrul Saatçi

E-mail:
e.saatci@iku.edu.tr

Received: 20.02.2020

Accepted: 17.03.2020

DOI: 10.5152/electrica.2020.20011

fractal structure has not been investigated to date. Therefore, the first step should be a complete understanding of the fractal properties of both respiratory signals and sounds, in which the correlation between the past, present, and future behaviors of signals is revealed. MFA explains the statistical properties of signals between the periods and within one period of the respiratory signals. Thus, using multifactal detrended fluctuation analysis (MF-DFA), this study aims to determine the mono or multifractal property of the respiratory signals.

Method

In this work, we used MF-DFA originally proposed in [13] and the implementation discussed in [14] to investigate the multifractal properties of both respiratory sounds and signals. According to MF-DFA, let $x[n]$ be a N point time series with Gaussian noise statistical properties. The steps comprising the method application are then summarized as follows:

Step 1: Computing the profile Y_i by integrating the time series:

$$Y_i = \sum_{n=1}^{i} [x[n] - \langle x \rangle] \tag{1}$$

where $\langle x \rangle$ is the mean of $x[n]$, and $i = 1, \mathrm{L}\ , N$. Basically, this step converts the statistical properties of time series from a Gaussian noise-like signal to a random walk-like signal (discrete-time counterpart of Brownian motion) because the MF-DFA method works on random walk-like signals.

Step 2: Dividing the profile Y_i into nonoverlapping scales of length s:

Using a rectangular window, profile Y_i is divided into nonoverlapping scales $s \in Z^+$. Segment $Y_v(i)$ of Y_i is then obtained for $v = 1, \cdots, 2N_s$. The length N of Y_i is not always an integer multiple of s; hence, Y_i is divided into $N_s \equiv \mathrm{int}(N/s)$ segments right from the beginning and the end of the sequence. The total number of the segments then becomes $2N_s$.

Step 3: Computing the local trend for each segment using least squares fit:

An m th-order polynomial $y_v(i)$ is then fitted to each segment $Y_v(i)$. Here, $y_v(i)$ is the m th-order polynomial fitted to the v th segment.

Step 4: Computing mean square fluctuations (variance):

This trend is removed in each segment v by subtracting the local trend $y_v(i)$ from the v th original profile $Y_v(i)$. The mean square fluctuations are then computed.

$$F^2(v,s) = \frac{1}{s} \sum_{i=1}^{s} [Y_v(i) - y_v(i)]^2 \tag{2}$$

Step 5: Computing the qth-order fluctuation function:

$$F_q(s) = \left\{ \frac{1}{2N_s} \sum_{v=1}^{2N_s} [F^2(v,s)]^{q/2} \right\}^{1/q} \tag{3}$$

where $q \in R$ is the order. The standard DFA procedure is obtained if $q = 2$. We examined how $F_q(s)$ changes based on different values of q with respect to s by repeating steps 2–5 for distinct values of s and q. In (3), N_s should be large; thus, s was forced to be sufficiently small to have statistically solid results. However, for the small s values, we may observe an overfitting in the polynomial curve fitting step. The literature recommends that s should change in the range of $m + 2 \le s < N/4$.

Step 6: Analyzing the scaling behavior of the q th-order fluctuation function.

To determine the scaling behavior of the fluctuation functions and to investigate the relationship between the curves, $F_q(s)$ is plotted versus scale s on a double logarithmic graph for selected q orders. In particular, the slopes of the curves are evaluated in terms of resemblance.

Considerations for MF-DFA Analysis

Before using the abovementioned method proposed in Ref. [13], we should consider the following points:

If the original time series $x[n]$ is long range power law correlated, then for large values of scale s, $F_q(s)$ increases and is expressed as a power law as (4):

$$F_q(s) \sim s^{h(q)} \tag{4}$$

where $h(q)$ is called a generalized Hurst exponent that is generally dependent on q. In a monofractal time series, $h(q)$ is independent from q. Moreover, in a stationary time series, $h(2)$ corresponds to the classical Hurst exponent.

If $x[n]$ is a zero-mean and normalized time series with a statistical property of stationarity, Step 3 is skipped, and the variance in (2) is computed using the consecutive segments of $Y_v(i)$. This method corresponds to standard fluctuation analysis.

$$F_{FA}^2(v,s) = \frac{1}{s} \sum_{i=1}^{s} [Y_v(i) - Y_{v-1}(i)]^2 \tag{5}$$

In Step 3, order m is selected using a trial and error method. For a biomedical time series, it generally changes in the range of $1 \le m < 3$.

The generalized Hurst exponent will be significantly altered by q if the small and large fluctuations are differently scaled. When one envisages the mean square fluctuations in (2) and the averaged fluctuation function in (3) for small time scale values s, the $F^2(v,s)$ values computed for the segments with small fluctuations dominate the average value $F_q(s)$ for $q<0$. However, the $F^2(v,s)$ values computed for the segments with large fluctuations dominate $F_q(s)$ for $q>0$; thus, $F_{q>0}(s) > F_{q<0}(s)$. If $F_q(s)$ is assumed to have a homogenous scaling behavior because of (4), in the double logarithmic plot of $F_q(s)$ versus s, the slope of $h(q)$ for $q<0$ will be greater than the slope of $h(q)$ for $q>0$, i.e., $h(q<0) > h(q>0)$.

Data Collection and Preprocessing

We acquired 22 different respiratory signals and sounds from 11 different subjects in the Department of Respiratory Medicine at Koc University Hospital. Table 1 lists the acquired respiratory signals and channel names. During data acquisition, the subjects were in an erect position and wore noise clips. They regularly inhaled and exhaled in a relaxed condition with a low flow for 60 s and in deep breath with a high flow for another 60 s. The respiratory signals were then digitized using a sampling frequency of 8000 Hz and a resolution of 16 bit using a commercial data acquisition (DAQ) card, and then stored in the computer. In the preprocessing step, discrete signals containing 480,000 sample points were separated into cycles comprising both inspiration and expiration phases. No filtering was applied to preserve all components in the signal and maintain the statistical properties, which are sensitive to the filtering process.

Table 1. Acquired Respiratory Signals

Lung sounds	Ch. 1–6: lung sounds	Multifractal
	Ch. 7: tracheal sound	Multifractal
Auxilary signals	Ch. 8: temperature of the breathing air	Multifractal
	Ch. 9: humidity of the breathing air	Multifractal
Respiratory signals	Ch. 10: airflow	Monofractal
	Ch. 11: mouth pressure	Multifractal
	Ch. 12: lung volume	Monofractal

Application of MF-DFA to Respiratory Signals and Sounds

MF-DFA is applicable to a time series having a random walk-like structure. Therefore, before multifractal analysis, the statistical properties of respiratory signals and sounds should be assessed. In Step 1, the abovementioned method converts Gaussian noise-like signals to random walk-like signals. As explained in [14], the method computes the Hurst exponent $h(2)$ for the signal. If $h(2)<1$, the signal is a Gaussian noise-like one; therefore, the abovementioned method is applied without any change. However, if the Hurst exponent $h(2)>1$, the signal is a random walk-like one. In this case, Step 1 is skipped, i.e., $Y_i = x[i]$, $i = 1,\mathrm{L}\ ,N$.

In each respiratory cycle, the number of samples varied between 9369 and 64180 samples. Thus, for the first analysis, where the fractal scaling properties are compared between breathing cycles, the time scale was changed from 64 ms ($s_{\min} = 512$ samples) to the quarter of the cycle length with a step size of 64 ms. For each cycle, the lengths N of the periods were different; thus, we had distinct numbers of segments $2N_s$ in Step 2. In the second analysis, where the fractal scaling properties were identified within the breathing cycle, a rectangular window with a length of 2048 sample divided the period into non-overlapped segments. In this case, the time scale was changed from 2 ($s_{\min} = 16$ samples) to 64 ms ($s_{\max} = 512$ samples). The fractal analysis within one period yielded scaling properties comparable between inspiration and expiration or between different parts of the period.

In the literature, during the curve fitting step, orders $m = 1, 2, \text{and } 3$ were normally used, and the generalized Hurst exponent successfully revealed the scaling properties. In this study, $m = 1$ was selected for all the simulations, and order q of the fluctuation function changed over the range $q = -10,\mathrm{L}\ ,10$, and the generalized Hurst exponent was calculated as explained in the Method section.

Results and Discussion

Figure 1 shows the Hurst exponent $h(2)$ values in each channel for all subjects as a box plot. The average Hurst exponent values calculated over all periods for all subjects were used in the figure. As shown in the figure, the Hurst exponent values of the lung sounds in channels 1–7 were <1, whereas those of the respiratory signals were >1. This result indicates that the lung sounds were Gaussian noise-like signals that should be con-

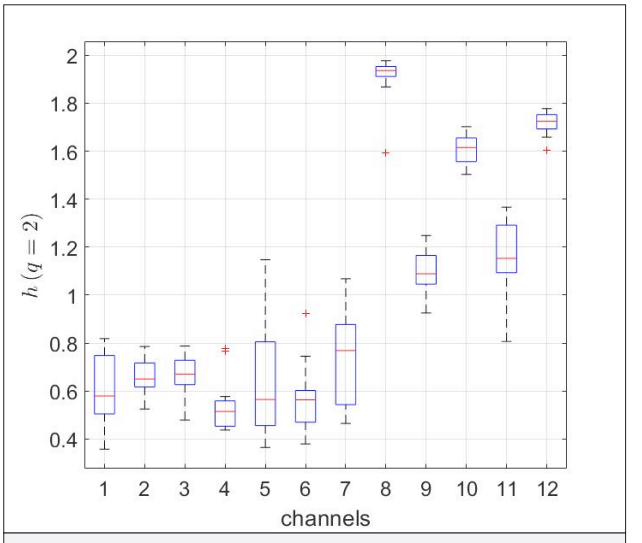

Figure 1. Box plot chart of the Hurst exponent $h(2)$ for each channel.

verted to random walk-like signals with the help of Step 1. Furthermore, the Hurst exponents of the respiratory sounds were >0.5, which statistically indicates that the respiratory sound signals have considerable memory. The temperature of breathing air, airflow, and lung volume signals in channels 8, 10, and 12 were random walk-like signals because the Hurst exponent values were >1. In channels 9 and 11, the humidity of breathing air and the mouth pressure signals were at the border. Furthermore, for most subjects, these signals showed random walk-like properties. However, for three (i.e., 10, 11, and 14) and four (i.e., 13, 14, 18, and 19) subjects, the humidity signal and the mouth pressure signal, respectively, were slightly <1, showing Gaussian noise-like properties. We demonstrated the results for only one patient in Figure 2 to investigate the deviations of the Hurst exponent values between periods in each channel for a chosen subject (Subject 22). The Hurst exponent values apparently demonstrated very minor differences between periods. Therefore, the Hurst exponent values between the periods did not supply the distinctive properties of the signals. Similar results were obtained from the other subjects' Hurst exponent values.

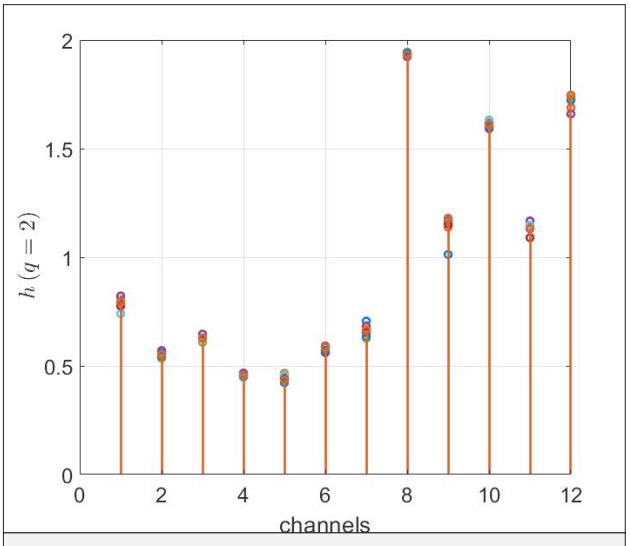

Figure 2. Deviation of the Hurst exponent $h(2)$ values between periods in each channel for Subject 22.

The other interesting investigation aimed to explore the changes in the Hurst exponent within each period. Figures 3a and b show the variation of the Hurst exponent calculated for the airflow and mouth pressure signals of Subject 22, respectively. Here, to segment the periods, 1024 points nonoverlapped rectangular windows were used. As explained earlier, the Hurst exponent was calculated for each segment. On the same figure, the original signal was plotted to demonstrate changes via inspiration and expiration. First, the Hurst exponent was nearly constant at ~1 for both signals. This result was expected because the signals changed slowly. Moreover, no significant difference was reported between inspiration and expiration,

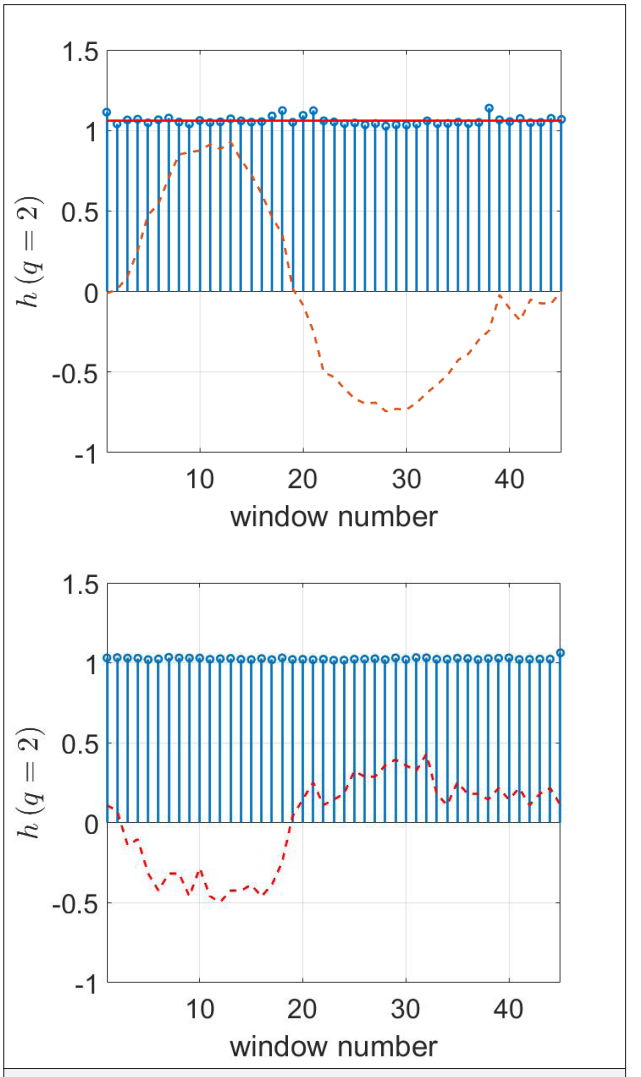

Figure 3. Variation of the Hurst exponent $h(2)$ calculated for the a) airflow and b) mouth pressure signals for Subject 22.

indicating that raw respiratory sounds and signals did not demonstrate statistical differences between inspiration and expiration in terms of fractal analysis. This result is very surprising because the dynamic relationship between these signals is different in both inspiration and expiration [15].

Finally, MFA was performed on the signals. Figures 4a and b show the first result from the analysis for Subject 22 and the fluctuation function $F_q(s)$ with respect to time scale s on double logarithmic scale for airflow signal and tracheal sounds, respectively. Figures 4a and b show the generalized Hurst exponent $h(q)$ versus order q for the same signals. Figure 4a shows that solid lines are linear fits to the data points of $F_q(s)$. The slopes of the lines for the orders $q = -10$, $q = 0$, and $q = 10$ are nearly constant (parallel lines). In other words, in this appointed scale range, the airflow signal has a monofractal scaling behavior . However, Figure 4b shows a multifractal scaling behavior of the tracheal sound signal. These results agree

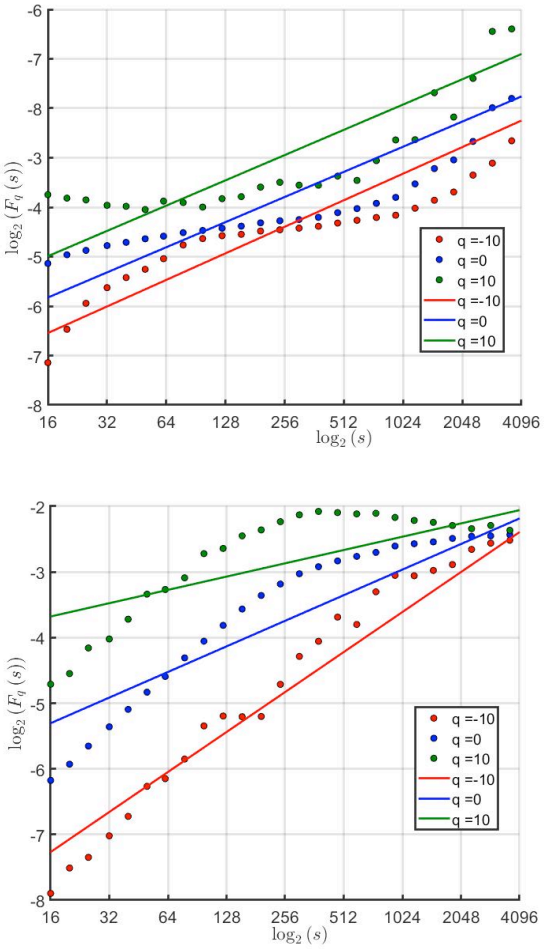

Figure 4. Fluctuation function $F_q(s)$ with respect to time scale s on the double logarithmic scale for the a) airflow signal and b) tracheal sounds.

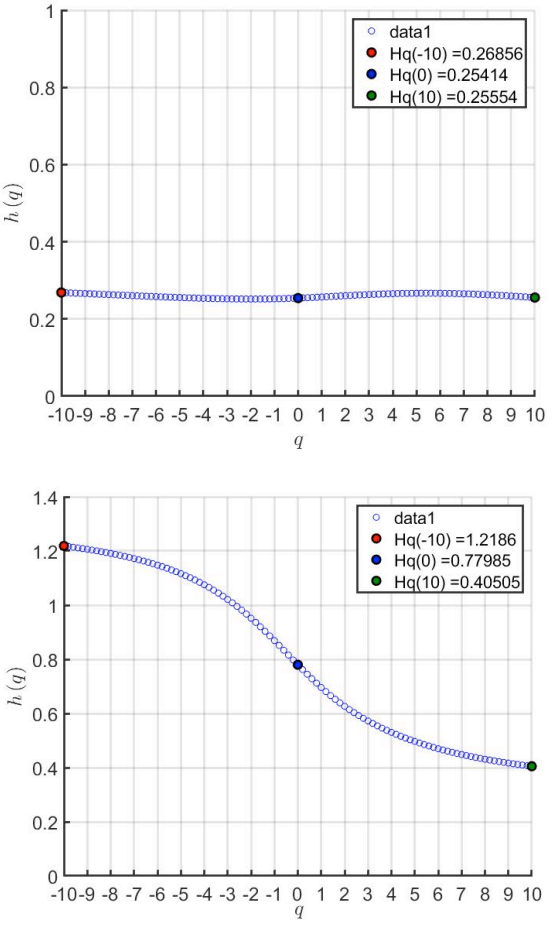

Figure 5. Generalized Hurst exponent $h(q)$ with respect to order q for the a) airflow signal and b) tracheal sounds.

with those obtained from Figures 5a and b. in Figure 5a, the generalized Hurst exponent was clearly nearly independent from order q, which is the definition of monofractality. However, Figure 5b shows that the generalized Hurst exponent varied by order q, which is an indication of multifractality.

Table I shows the results for all channels. Furthermore, we observed that similar results were obtained for all subjects and all periods. Thus, we confidently conclude that the multifractal behavior deviates only between the channels (signals) and does not change between the periods. However, the variations because of the pathological cases of the signals remain to be further analyzed.

Conclusion

In this study, to reveal the fractal scaling properties of the respiratory sounds and signals, we successfully used MF-DFA proposed in the literature. The fractal scaling properties are associated with statistical properties of signals; hence, the results provided valuable information about statistical nature of signals. The respiratory system is well known to possess a fractal geometry, which facilitates signals having fractal scaling properties. However, a detailed monofractal vs multifractal analysis was performed, and the results demonstrated both respiratory sounds and signals are generally multifractal signals, except for the airflow and the lung volume. During respiratory tests, the probability density function of multifractal signals is scale variant, and this result is very significant because while diagnosing respiratory diseases, , airway resistance and lung compliance are estimated using acquired respiratory signals and lung models. This method of identifying respiratory parameters requires a stationary relationship between signals. However, both the multifractal property of the mouth pressure and the monofractal property of the airflow indicate that a statistically dynamic relationship exists between signals. For this purpose, one should consider the productive connection between respiratory signals and respiratory system to search for parameters or features for diagnosis.

Ethics Committee Approval: Ethics committee approval was received for this study from the Ethical Committee of Istanbul Kultur University (2018.01/01.04.2018).

Peer-review: Externally peer-reviewed.

Conflict of Interest: The authors declared no conflicts of interest.

Financial Disclosure: This study was partially supported by the Research Fund of Istanbul Kultur University, Grant No: IKU-BAP1801.

References

1. P. Castiglioni, G. Parati, A. Civijian, L. Quintin and M. Di Rienzo, "Local Scale Exponents of Blood Pressure and Heart Rate Variability by Detrended Fluctuation Analysis", IEEE Trans Biomed Eng, vol. 56, no. 3, pp. 675-684, 2009.
2. D. Abasolo, R. Horneo, J. Escudero and P. Espino, "A study on the Possible Usefulness of Detrended Fluctuation Analysis of the Electroencephalogram Background Activity in Alzheimer's disease", IEEE Trans Biomed Eng, vol. 55, no.9, pp. 2171-2179, 2008.
3. S. Chatterjee, S. Pratiher, R. Bose, "Multifractal Detrended Fluctuation Analysis Based Novel Feature Extraction Technique for Autometed Detection of Focal and Non-Focal Electroencephalogram Signals", IET Sci Meas Technol, vol. 11, no. 8, pp. 1014-1021, 2017.
4. S. P. Chakravarty, S. Chakraborty, "Fractal analysis related to tumour growth in lungs: a review", 2017 Fourth International Conference on Image Information Processing (ICIIP), India, 2017, pp. 422-425.
5. J. Gnitecki, Z. Moussavi, "The fractality of lung sounds: a comparison of three waveform fractal dimension algorithms", Chaos Solitons Fractals, vol. 26, pp. 1065-1072, 2005.
6. C. M. Ionescu, W. Kosinski, R. De Keyser, "Viscoelasticity and fractal structure in a model of human lungs", Arch Mech, vol. 97, pp. 21-48, 2010.
7. K. L. Uahabi and M. Atounti, "New approach to the calculation of fractal dimension of the lungs", Annals Unive. Craiova, Mathe and Comp. Scie, vol. 44, no. 1, pp. 78-86, 2017.
8. A. Rizal, R. Hidayat and H. A. Nugroho, "Fractal Dimension for lung sound classification in multiscale scheme", J Comp. Scie, vol. 14, no. 8, pp. 1081-1096, 2018.
9. J. Gnitecki, Z. Moussavi, H. Pasterkamp, "Classification of lung sounds during bronchial provocation using waveform fractal dimensions", 26th Annual International Conference of the IEEE Engineering in Medicine and Biology Society, San Francisco, USA, 2004, pp. 1-4.
10. L. J. Hadjileontiadis, I. T. Rekanos, "Detection of explosive lung and bowel Sounds by means of fractal dimension", IEEE Sig Proce Letters, vol. 10, no. 10, pp. 311-314, 2003.
11. M. Akay, E. H. Mulder, "Effects of maternal alcohol intake on fractal properties in human fetal breathing dynamics, IEEE Trans Biomed Eng, vol. 45, no. 9, pp. 1097-1102, 1998.
12. J. Gnitecki, Z. Moussavi, "Variance fractal dimension trajectory as a tool for heart sound localization in lung sounds recordings", 25th Annual International Conference of the IEEE Engineering in Medicine and Biology Society, Cancun, Mexico, 2003, pp. 2420-2423.
13. J. W. Kantelhardt, S. A. Zschiegner, E. Koscielny-Bunde, S. Havlin, A. Bunde and H. E. Stanley, "Multifractal detrended fluctuation analysis of nonstationary time series", Physica A, vol. 316, pp. 87-114, 2002.
14. E. A. F. Ihlen, "Introduction to multifractal detrended fluctuation analysis in Matlab", Front Physiol, vol. 3, no. 141, pp. 1-18, 2012.
15. E. Saatci, "Correlation analysis of respiratory signals by using parallel coordinate plots", Comp Method and Prog in Biomed, vol. 153, pp. 41-51, 2018.

Ertugrul Saatci received the B.S. and M.S. degree from Istanbul University, Istanbul, Turkey, in 1993 and 1996, respectively, and Ph.D. degree from London South Bank University in 2003. He is currently an Assistant Professor at Department of Electrical and Electronic Engineering, Istanbul Kultur University. His major research interests lie in the areas of signal and image processing, biometrics, biomedical signal processing and cellular neural networks.

Esra Saatci received the B.Sc. (1993) and Ph.D. (2009) degrees in electronic and biomedical engineering from Istanbul University, Turkey respectively; and M.Sc. (1995) degree in biomedical engineering from University of Surrey, UK. She worked for five years at respiratory and anesthesia instrumentation companies between 1995 and 1999 in Istanbul. She was a research assistant in mechanical engineering department at Kings College London between 2000 and 2004; and in electrical & electronics engineering department at Istanbul Kültür University between 2004 and 2009. Since 2009, she is an Assitant Professor at the Deparment of Electrical & Electronics Engineering, Istanbul Kültür University. Her current research interests include statistical signal processing with applications of biomedical signals, respiratory models and respiratory signal processing.